

# $\Omega^-$ and $\bar{\Omega}^+$ production in central Pb+Pb collisions at 40 and 158A GeV

C. Alt,<sup>9</sup> T. Anticic,<sup>21</sup> B. Baatar,<sup>8</sup> D. Barna,<sup>4</sup> J. Bartke,<sup>6</sup> L. Betev,<sup>9,10</sup> H. Białkowska,<sup>19</sup> A. Billmeier,<sup>9</sup> C. Blume,<sup>9</sup> B. Boimska,<sup>19</sup> M. Botje,<sup>1</sup> J. Bracinik,<sup>3</sup> R. Bramm,<sup>9</sup> R. Brun,<sup>10</sup> P. Bunčić,<sup>9,10</sup> V. Cerny,<sup>3</sup> P. Christakoglou,<sup>2</sup> O. Chvala,<sup>15</sup> J.G. Cramer,<sup>17</sup> P. Csató,<sup>4</sup> N. Darmenov,<sup>18</sup> A. Dimitrov,<sup>18</sup> P. Dinkelaker,<sup>9</sup> V. Eckardt,<sup>14</sup> G. Farantatos,<sup>2</sup> D. Flierl,<sup>9</sup> Z. Fodor,<sup>4</sup> P. Foka,<sup>7</sup> P. Freund,<sup>14</sup> V. Friese,<sup>7</sup> J. Gál,<sup>4</sup> M. Gaździcki,<sup>9,12</sup> G. Georgopoulos,<sup>2</sup> E. Gładysz,<sup>6</sup> K. Grebieszko,<sup>20</sup> S. Hegyi,<sup>4</sup> C. Höhne,<sup>13</sup> K. Kadija,<sup>21</sup> A. Karev,<sup>14</sup> M. Kliemant,<sup>9</sup> S. Kniege,<sup>9</sup> V.I. Kolesnikov,<sup>8</sup> T. Kollegger,<sup>9</sup> E. Kornas,<sup>6</sup> R. Korus,<sup>12</sup> M. Kowalski,<sup>6</sup> I. Kraus,<sup>7</sup> M. Kreps,<sup>3</sup> M. van Leeuwen,<sup>1</sup> P. Lévai,<sup>4</sup> L. Litov,<sup>18</sup> B. Lungwitz,<sup>9</sup> M. Makariev,<sup>18</sup> A.I. Malakhov,<sup>8</sup> C. Markert,<sup>7</sup> M. Mateev,<sup>18</sup> B.W. Mayes,<sup>11</sup> G.L. Melkumov,<sup>8</sup> C. Meurer,<sup>9</sup> A. Mischke,<sup>7</sup> M. Mitrovski,<sup>9</sup> J. Molnár,<sup>4</sup> St. Mrówczyński,<sup>12</sup> G. Pála,<sup>4</sup> A.D. Panagiotou,<sup>2</sup> D. Panayotov,<sup>18</sup> A. Petridis,<sup>2</sup> M. Pikna,<sup>3</sup> L. Pinsky,<sup>11</sup> F. Pühlhofer,<sup>13</sup> J.G. Reid,<sup>17</sup> R. Renfordt,<sup>9</sup> A. Richard,<sup>9</sup> C. Roland,<sup>5</sup> G. Roland,<sup>5</sup> M. Rybczyński,<sup>12</sup> A. Rybicki,<sup>6,10</sup> A. Sandoval,<sup>7</sup> H. Sann,<sup>7,\*</sup> N. Schmitz,<sup>14</sup> P. Seyboth,<sup>14</sup> F. Siklér,<sup>4</sup> B. Sitar,<sup>3</sup> E. Skrzypczak,<sup>20</sup> G. Stefanek,<sup>12</sup> R. Stock,<sup>9</sup> H. Ströbele,<sup>9</sup> T. Susa,<sup>21</sup> I. Szentpétery,<sup>4</sup> J. Sziklai,<sup>4</sup> T.A. Trainor,<sup>17</sup> D. Varga,<sup>4</sup> M. Vassiliou,<sup>2</sup> G.I. Veres,<sup>4,5</sup> G. Vesztergombi,<sup>4</sup> D. Vranić,<sup>7</sup> A. Wetzler,<sup>9</sup> Z. Włodarczyk,<sup>12</sup> I.K. Yoo,<sup>16</sup> J. Zaraneck,<sup>9</sup> and J. Zimányi<sup>4</sup>

(The NA49 collaboration)

<sup>1</sup>NIKHEF, Amsterdam, Netherlands.

<sup>2</sup>Department of Physics, University of Athens, Athens, Greece.

<sup>3</sup>Comenius University, Bratislava, Slovakia.

<sup>4</sup>KFKI Research Institute for Particle and Nuclear Physics, Budapest, Hungary.

<sup>5</sup>MIT, Cambridge, USA.

<sup>6</sup>Institute of Nuclear Physics, Cracow, Poland.

<sup>7</sup>Gesellschaft für Schwerionenforschung (GSI), Darmstadt, Germany.

<sup>8</sup>Joint Institute for Nuclear Research, Dubna, Russia.

<sup>9</sup>Fachbereich Physik der Universität, Frankfurt, Germany.

<sup>10</sup>CERN, Geneva, Switzerland.

<sup>11</sup>University of Houston, Houston, TX, USA.

<sup>12</sup>Institute of Physics Świetokrzyska Academy, Kielce, Poland.

<sup>13</sup>Fachbereich Physik der Universität, Marburg, Germany.

<sup>14</sup>Max-Planck-Institut für Physik, Munich, Germany.

<sup>15</sup>Institute of Particle and Nuclear Physics, Charles University, Prague, Czech Republic.

<sup>16</sup>Department of Physics, Pusan National University, Pusan, Republic of Korea.

<sup>17</sup>Nuclear Physics Laboratory, University of Washington, Seattle, WA, USA.

<sup>18</sup>Atomic Physics Department, Sofia University St. Kliment Ohridski, Sofia, Bulgaria.

<sup>19</sup>Institute for Nuclear Studies, Warsaw, Poland.

<sup>20</sup>Institute for Experimental Physics, University of Warsaw, Warsaw, Poland.

<sup>21</sup>Rudjer Boskovic Institute, Zagreb, Croatia.

Results are presented on  $\Omega$  production in central Pb+Pb collisions at 40 and 158A GeV beam energy. Given are transverse-mass spectra, rapidity distributions, and total yields for the sum  $\Omega^- + \bar{\Omega}^+$  at 40A GeV and for  $\Omega^-$  and  $\bar{\Omega}^+$  separately at 158A GeV. The yields are strongly under-predicted by the string-hadronic UrQMD model and agree with predictions from a hadron gas model assuming strangeness under-saturation.

PACS numbers: 25.75.-q

The measurement of multi-strange particles is of particular interest in heavy ion collisions at ultra-relativistic energies. One important aspect is the observation that the inverse slope parameter  $T$  of the  $\Omega$   $m_t$ -spectrum [1] is significantly smaller than the expectation from a linear mass dependence of  $T$ , as naively implied by the presence of radial flow. This leads to the hypothesis that multi-strange hyperons are not affected by the pressure generated by the hadronic matter in later stages of the reaction [2]. Originally, the increase of the production of multi-strange particles as compared to elementary hadron-hadron collisions has been suggested as

a signature of quark-gluon plasma formation [3]. However, existing experimental data on  $\Xi$  and  $\Lambda$  production at lower beam energies [4, 5] exhibit a much stronger strangeness enhancement than observed at top SPS energies. Generally, it is found that the abundances of strange particles are close to those calculated in statistical models assuming the creation of an equilibrated hadron gas [6]. In a hadronic environment, as realized at lower beam energies, this equilibration is generally difficult to achieve. At larger energy densities, when the hadronic system might be close to the QGP phase boundary, multi-particle fusion processes can be sufficient for

fast equilibration [7]. However, there exists no dynamic explanation in a hadronic scenario at lower energy densities. The present measurement of  $\Omega$  at 40A GeV provides an important test for these models. Recent results on the energy dependence of the ratio  $\langle K^+ \rangle / \langle \pi \rangle$  [8, 9] indicate a sharp maximum of the relative strangeness production at a beam energy of 30A GeV. This anomaly can be interpreted as a signal for the onset of deconfinement [10] and might be reflected in the energy dependence of multi-strange particle production.

The data were taken with the NA49 large acceptance hadron spectrometer at the CERN SPS. With this detector, tracking is performed by four large-volume TPCs. A measurement of the specific energy loss  $dE/dx$  provides particle identification at forward rapidities. Time-of-flight detectors improve the particle identification at mid-rapidity. Centrality selection is based on a measurement of the energy deposited in a forward calorimeter by the projectile spectators. A detailed description of the apparatus can be found in [11].

We present in this paper an analysis of two samples of central Pb+Pb events taken at beam energies of 40 and 158A GeV in the years 1999 and 2000, respectively. About  $5.8 \times 10^5$  events were recorded at 40A GeV with a centrality selection of 7.2% of the total inelastic cross section corresponding, on average, to  $\langle N_w \rangle = 349$  wounded nucleons [12]. At 158A GeV,  $2.8 \times 10^6$  events were taken at 23.5% centrality corresponding to  $\langle N_w \rangle = 262$ .

The  $\Omega$  were identified in the decay channel  $\Omega \rightarrow \Lambda K$ ,  $\Lambda \rightarrow p\pi$  (68% branching fraction). To reconstruct the  $\Omega^-$  ( $\bar{\Omega}^+$ ), the  $\Lambda$  ( $\bar{\Lambda}$ ) candidates were selected in an invariant-mass window of 1.101–1.131 GeV/ $c^2$  and combined with all negatively (positively) charged tracks in the event. The same procedure as in the  $\Xi$  analysis of [13] was used to identify the secondary vertex of the  $\Omega$  decay.

To reduce the combinatorial background several cuts were applied. Identification of the (anti-)protons by  $dE/dx$  in the TPCs reduced the contribution from fake  $\Lambda$  ( $\bar{\Lambda}$ ). The measured  $dE/dx$  was required to be within 3.5 standard deviations from the predicted Bethe-Bloch value. Likewise an enriched kaon sample was extracted from the charged tracks. A further background reduction was achieved by requiring a minimal distance of 25 cm in the beam direction between the  $\Omega$  decay vertex and the target position. The  $\Omega$  candidates were extrapolated back to the target plane to obtain the transverse coordinates  $b_x$  (magnetic bending plane) and  $b_y$  of the impact point with respect to the primary interaction vertex. To reject non-vertex candidates, cuts of  $|b_x| < 0.5$  cm and  $|b_y| < 0.25$  cm were applied. Kaons from the primary vertex were excluded by imposing a cut of  $|b_y| > 1.0$  cm on the kaon tracks. In addition,  $|b_y| > 0.4$  cm was required for the  $\Lambda$  candidates at 40A GeV. With these cuts an acceptable separation of signal and background was achieved for  $\Omega$  transverse momenta above 0.9 GeV/ $c$ .

In Fig. 1 the invariant-mass distributions of the  $\Omega^-$

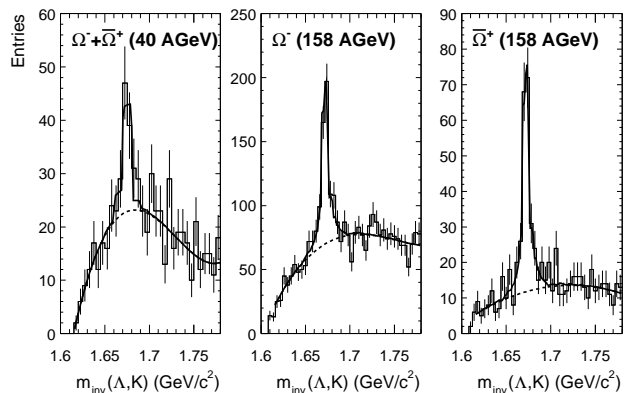


FIG. 1: The invariant-mass distributions of  $\Omega^-$  and  $\bar{\Omega}^+$  candidates. Left: summed distribution of  $\Lambda K^-$  and  $\bar{\Lambda} K^+$  pairs at 40A GeV. Middle:  $\Lambda K^-$  pairs at 158A GeV. Right:  $\bar{\Lambda} K^+$  pairs at 158A GeV. The full curves represent a fit to signal and background described in the text. The dashed curves show the background contribution.

and  $\bar{\Omega}^+$  candidates are shown. Note that the available statistics at 40A GeV is not sufficient to separately analyze the  $\Omega^-$  and  $\bar{\Omega}^+$  [14]. The kinematic range covered by the spectra is  $p_t > 0.9$  GeV/ $c$  in transverse momentum and  $-0.5 < y < 0.5$  ( $-1.0 < y < 1.0$ ) in rapidity for the 40 (158)A GeV data. Clear signals are observed at the  $\Omega$  mass of  $m_0 = 1672.5$  MeV/ $c^2$  [15] with a resolution of 5 and 4 MeV/ $c^2$  at 40 and 158A GeV, respectively.

The spectra were fitted to the sum of a polynomial background and a signal distribution, determined from the simulation described below. The raw  $\Omega$  yield is obtained by subtracting the fitted background in a mass window of  $\pm 7$  MeV/ $c^2$  around the nominal  $\Omega$  mass.

Detailed simulations were made to correct the yields for geometrical acceptance and losses in the reconstruction. For this purpose, a sample of  $\Omega$  was generated in the full phase space accessible to the experiment. The Geant 3.21 package [16] was used to track the generated  $\Omega$  and their decay particles through a detailed description of the NA49 detector geometry. Dedicated NA49 software was used to simulate the TPC response taking into account all known detector effects. The simulated signals were added to those of real events and subjected to the same reconstruction procedure as the experimental data. The acceptance and efficiency were calculated in bins of  $p_t$  and  $y$  as the fraction of the generated  $\Omega$  which traverse the detector, survive the reconstruction and pass the analysis cuts. This fraction amounts to 0.2–0.5%, depending on  $p_t$  and  $y$ .

The systematic uncertainties are dominated by the background subtraction method and by imperfections in the simulation. By varying the analysis strategy and the cuts applied, a systematic error of 10% is estimated in the transverse-mass region  $(m_t - m_0) > 0.3$  GeV. At lower  $m_t$  this error is about 25%.

In Fig. 2 the transverse-mass spectra of the  $\Omega$  are

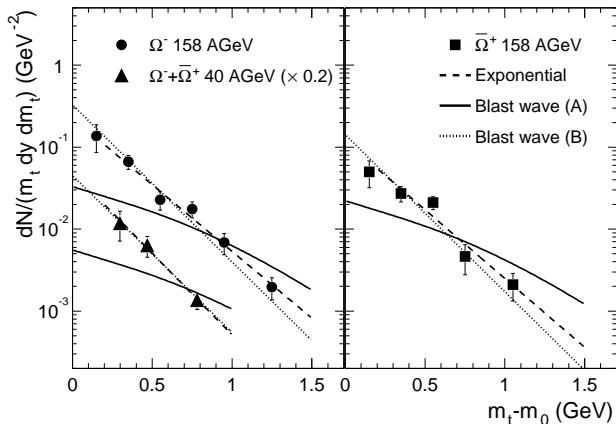


FIG. 2: The transverse-mass spectra of  $\Omega^-$  and  $\bar{\Omega}^+$  at mid-rapidity. Left:  $\Omega^- + \bar{\Omega}^+$  at 40A GeV (triangles) and  $\Omega^-$  at 158A GeV (circles). Right:  $\bar{\Omega}^+$  at 158A GeV. The errors shown are statistical only. The dashed curve shows the exponential fit described in the text. The full and dotted curves show a model including transverse expansion with two different sets of parameters.

shown integrated over the range  $\pm 0.5$  (40A GeV) and  $\pm 1$  (158A GeV) around mid-rapidity. The transverse-mass spectra were fitted to an exponential function

$$\frac{dN}{m_t dm_t dy} \propto \exp\left(-\frac{m_t}{T}\right) \quad (1)$$

in the range  $(m_t - m_0) > 0.2$  GeV. The results are plotted in Fig. 2 (dashed curves) and the inverse slope parameters  $T$  are listed in Table I. No significant difference

TABLE I: The inverse slope parameter  $T$  (MeV), the width  $\sigma$  of the rapidity distribution, the mid-rapidity yield  $dN/dy$  and the total yield  $\langle N \rangle$  of  $\Omega$  production at 40 and 158A GeV. The first error is statistical and the second systematic.

	40A GeV $\Omega^- + \bar{\Omega}^+$	158A GeV $\Omega^-$	158A GeV $\bar{\Omega}^+$
$T$	$218 \pm 39 \pm 39$	$267 \pm 26 \pm 10$	$259 \pm 35 \pm 18$
$\sigma$	$0.6 \pm 0.1 \pm 0.1$	$1.2 \pm 0.4 \pm 0.2$	$1.0 \pm 0.4 \pm 0.2$
$dN/dy$	$0.10 \pm 0.02 \pm 0.02$	$0.14 \pm 0.05 \pm 0.01$	$0.07 \pm 0.02 \pm 0.01$
$\langle N \rangle$	$0.20 \pm 0.03 \pm 0.04$	$0.37 \pm 0.07 \pm 0.03$	$0.17 \pm 0.03 \pm 0.02$

can be observed in the shape of the  $\Omega^-$  and  $\bar{\Omega}^+$  spectra at 158A GeV. The inverse slope parameters are close to the values obtained by the WA97 and NA57 collaborations [1, 17]. The inverse slope parameter at 40A GeV is somewhat lower but, within errors, compatible with the 158A GeV result.

To investigate whether the  $\Omega$  decouples earlier from the fireball than lighter hadrons, we use a hydrodynamical model which assumes a transversely expanding emission

source [18]. The parameters of this model are the freeze-out temperature  $T_f$  and the transverse flow velocity  $\beta_s$  at the surface. Assuming a linear radial velocity profile  $\beta_t(r) = \beta_s r/R$ , which is motivated by hydrodynamical calculations, the  $m_t$ -spectrum can be computed from

$$\frac{dN}{m_t dm_t dy} \propto \int_0^R r dr m_t I_0\left(\frac{p_t \sinh \rho}{T_f}\right) K_1\left(\frac{m_t \cosh \rho}{T_f}\right), \quad (2)$$

where  $R$  is the radius of the source and  $\rho = \tanh^{-1} \beta_t$  is the boost angle. The full curve (A) in Fig. 2 shows the result of a calculation with  $T_f = 90$  MeV and an average flow velocity  $\langle \beta_t \rangle = 0.5$ . These parameters were obtained from a simultaneous fit of the model to the  $m_t$ -spectra of  $K^+$ ,  $K^-$ ,  $p$ ,  $\bar{p}$ ,  $\phi$ ,  $\Lambda$ , and  $\bar{\Lambda}$ , all measured by NA49 at 158A GeV [4, 8, 19, 20]. The dotted curve (B) is calculated with  $T_f = 170$  MeV and  $\langle \beta_t \rangle = 0.2$ , obtained from a fit to  $J/\psi$  and  $\psi'$  spectra [21]. The disagreement of curve (A) and the agreement of curve (B) with the data suggest that, given the model, the freeze-out conditions of the  $\Omega$  are similar to those of the  $J/\psi$  or  $\psi'$  but are different from those of the lighter hadrons. However, this difference is less pronounced when a fixed expansion velocity is used instead of a velocity profile [22].

The parameterizations of Eqs. (1) and (2) were used to extrapolate the  $\Omega$  yields into the unmeasured regions of  $m_t$ . Assuming that the shape of the  $m_t$ -distribution does not depend on rapidity, extrapolation factors of 2.3 (2.2) at 40 (158)A GeV were obtained from fits to the summed  $\Omega^-$  and  $\bar{\Omega}^+$  data. A systematic uncertainty of 6% is due to the choice of parameterization.

The extrapolated  $\Omega$  yields at 40 and 158A GeV are shown in Fig. 3 as a function of rapidity. All spectra can be described by a Gaussian with zero mean and a width  $\sigma$  obtained from a fit to the data, see Table I. The widths of the  $\Omega^-$  and  $\bar{\Omega}^+$  spectra at 158A GeV are compatible but are both significantly larger than the width measured at 40A GeV. Also given in Table I are the mid-rapidity yields  $dN/dy$  ( $-0.5 < y < 0.5$ ) and the total yields  $\langle N \rangle$  obtained from extrapolation of the rapidity spectra into the unmeasured region using the Gaussian fits. The mid-rapidity yields are slightly below the values given by the NA57 collaboration [23], however, they agree within statistical errors, if the difference in the centrality selection at 158A GeV is taken into account.

In the following we denote by  $\langle \Omega \rangle$  the sum of the total  $\Omega^-$  and  $\bar{\Omega}^+$  yields and by  $\langle \pi \rangle$  the total charged pion yields from [8], multiplied by a factor 1.5. The pion yields at 158A GeV were scaled by the ratio of the numbers of wounded nucleons to account for the difference in the centrality selection of the pion and the  $\Omega$  measurement. In Fig. 4 is shown the ratio  $\langle \Omega \rangle / \langle \pi \rangle$  as function of the center-of-mass energy. It is seen that this ratio tends to increase with energy. The ratio is clearly under-predicted by the UrQMD string-hadronic model [24] as shown by the dashed curve in Fig. 4. A better description of the

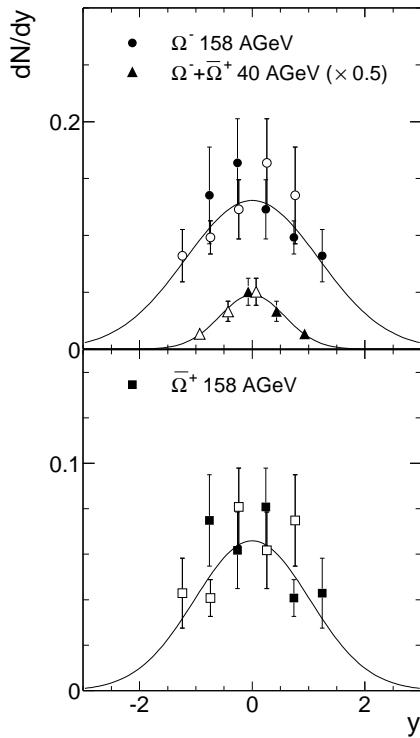


FIG. 3: The rapidity dependence of  $\Omega$  production in central Pb+Pb collisions. Top:  $\Omega^- + \Omega^+$  at 40 AGeV (triangles) and  $\Omega^-$  at 158 AGeV (circles). Bottom:  $\bar{\Omega}^+$  at 158 AGeV. The errors shown are statistical only. The open symbols show the measured points (full symbols) reflected around mid-rapidity. The curves correspond to Gaussian fits to the data.

158 A GeV data is provided by RQMD version 2.3 including the color rope mechanism [25].

On the other hand, the data are close to the predictions of statistical hadron gas models which use a grand canonical ensemble. In these models, the chemical freeze-out temperature and the baryonic chemical potential are fitted to the yields of other measured hadrons. The hadron gas model of [26] (labeled B in Fig. 4) introduces in addition a strangeness under-saturation factor  $\gamma_s$  as a parameter in the fit. The present measurement at 158 A GeV seems to favor this model, compared to that of [27] (labeled A in Fig. 4) which does not allow for strangeness under-saturation ( $\gamma_s = 1$  for all energies). The observation that  $\Omega$  production seems to be close to phase-space saturation at low SPS energies but under-saturates at the highest SPS energy is in line with a similar behavior of the kaon excitation function in the same energy regime [9]. This may indicate that the observed anomalous energy dependence of the relative strangeness yield, possibly caused by the onset of deconfinement at the low SPS energies [10], is consistent with the energy dependence of the ratio of multi-strange hadron to pion production.

In summary, NA49 has performed a measurement of

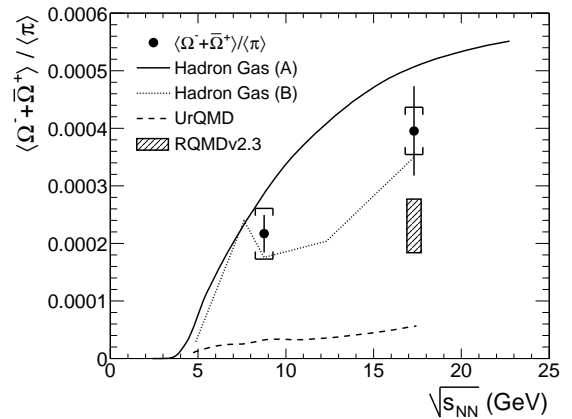


FIG. 4: The ratio  $\langle\Omega\rangle/\langle\pi\rangle$  (see text) versus the center-of-mass energy. Statistical errors are shown as lines, while the brackets denote the systematic errors. The dashed curve shows the prediction from the hadronic string model UrQMD [24] and the gray box that of RQMD [25]. A hadron gas model without strangeness suppression [27] is shown by the full curve. The dotted lines connect the predictions of [26] including strangeness suppression.

$\Omega$  production in central Pb+Pb reactions over a wide region of phase space. At a beam energy of 158 A GeV the available statistics allowed to separately analyze  $\Omega^-$  and  $\bar{\Omega}^+$ . The shapes of the transverse-mass spectra at this energy reveal no difference between  $\Omega^-$  and  $\bar{\Omega}^+$  and are in agreement with previous results by WA97 and NA57. In the framework of a hydrodynamical model, the data favor a low transverse expansion velocity and high freeze-out temperature as has also been observed for  $J/\psi$  and  $\psi'$ . The rapidity spectra of the  $\Omega$ , which have not been measured before in any kind of reaction system, are compatible with a Gaussian shape. The widths for  $\Omega^-$  and  $\bar{\Omega}^+$  appear to be similar. The yields are strongly under-predicted by the string-hadronic UrQMD model. The data agree with predictions from a hadron-gas model assuming strangeness under-saturation.

**Acknowledgments:** This work was supported by the US Department of Energy Grant DE-FG03-97ER41020/A000, the Bundesministerium für Bildung und Forschung, Germany, the Polish State Committee for Scientific Research (2 P03B 130 23, SPB/CERN/P-03/Dz 446/2002-2004, 2 P03B 04123), the Hungarian Scientific Research Fund, OTKA (T032648, T032293, T043514, F034707), the Polish-German Foundation, and the Korea Research Foundation Grant (KRF-2003-070-C00015).

\* deceased

[1] F. Antinori et al. [WA97 Collaboration], Eur. Phys. J. C **14**, 633 (2000).

- [2] H. van Hecke, H. Sorge, and N. Xu, Phys. Rev. Lett. **81**, 5764 (1998).
- [3] J. Rafelski and B. Müller, Phys. Rev. Lett. **48**, 1066 (1982).
- [4] T. Anticic et al. [NA49 Collaboration], Phys. Rev. Lett. **93**, 022302 (2004).
- [5] P. Chung et al. [E895 Collaboration], Phys. Rev. Lett. **91**, 202301 (2003).
- [6] F. Becattini, J. Cleymans, A. Keranen, E. Suhonen, and K. Redlich, Phys. Rev. **C 64**, 024901 (2001).
- [7] P. Braun-Munzinger, J. Stachel, and C. Wetterich, Phys. Lett. **B 596**, 61 (2004).
- [8] S.V. Afanasiev et al. [NA49 Collaboration], Phys. Rev. **C 66**, 054902 (2002).
- [9] M. Gaździcki et al. [NA49 Collaboration], J. Phys. **G 30**, 701 (2004).
- [10] M. Gaździcki and M.I. Gorenstein, Acta Phys. Polon. **B 30**, 2705 (1999).
- [11] S.V. Afanasiev et al. [NA49 Collaboration], Nucl. Instrum. Meth. **A 430**, 210 (1999).
- [12] A. Białas, M. Błeszyński, and W. Czyż, Nucl. Phys. **B 111**, 461 (1976).
- [13] S.V. Afanasiev et al. [NA49 Collaboration], Phys. Lett. **B 538**, 275 (2002).
- [14] M. Mitrovski, Diploma Thesis, University of Frankfurt (2004).
- [15] K. Hagiwara et al. (Particle Data Group), Phys. Rev. **D 66**, 010001 (2002).
- [16] Geant—Detector Description and Simulation Tool, CERN Program Library Long Writeup W5013.
- [17] F. Antinori et al., J. Phys. **G 30**, 823 (2004).
- [18] E. Schnedermann and U. Heinz, Phys. Rev. **C 50**, 1675 (1994).
- [19] T. Anticic et al. [NA49 Collaboration], Phys. Rev. **C 69**, 024902 (2004).
- [20] S.V. Afanasiev et al. [NA49 Collaboration], Phys. Lett. **B 491**, 59 (2000).
- [21] M.I. Gorenstein, K.A. Bugaev, and M. Gaździcki, Phys. Rev. Lett. **88**, 132301 (2002).
- [22] M. van Leeuwen et al. [NA49 Collaboration], Nucl. Phys. **A 715**, 161c (2003).
- [23] F. Antinori et al., Phys. Lett. **B 595**, 68 (2004).
- [24] M. Bleicher et al., J. Phys. **G 25**, 1859 (1999) and private communication.
- [25] U. Heinz, J. Sollfrank, H. Sorge, and N. Xu, Phys. Rev. **C 59**, 1637 (1999).
- [26] F. Becattini, M. Gaździcki, A. Keränen, J. Manninen, and R. Stock, Phys. Rev. **C 69**, 024905 (2004).
- [27] P. Braun-Munzinger, J. Cleymans, H. Oeschler, and K. Redlich, Nucl. Phys. **A 697**, 902 (2002) and private communication.